

Clarifying the Molecular Weight Dependence of the Segmental Dynamics of Polybutadiene

R. B. Bogoslovov,[†] T. E. Hogan,[‡] and C. M. Roland^{*†}[†]Naval Research Laboratory, Code 6120, Washington, D.C. 20375-5342, and [‡]Bridgestone Americas, Center for Research and Technology, 1200 Firestone Parkway, Akron, Ohio 44317-0001

Received December 7, 2009; Revised Manuscript Received February 16, 2010

ABSTRACT: A series of 1,4-polybutadienes of varying molecular weight, both monodisperse and having broad or bidisperse molecular weight distributions, were studied using dielectric relaxation. The glass transition temperature, T_g , and the T_g -normalized temperature dependence of the segmental relaxation times, τ_α , varied monotonically with number-average molecular, M_n . Polydispersity significantly affects neither T_g nor the shape of the loss peak; the segmental relaxation dispersion is determined solely by M_n , even when the distribution of chain lengths spans molecular weights over which T_g varies. However, there is a small but significant influence of polydispersity on the T -dependence of the relaxation times, manifested as greater fragility in samples having bimodal molecular weight distributions. Properties of the prominent Johari–Goldstein (JG) secondary relaxation in 1,4-polybutadiene were measured and found to be qualitatively in accord with predictions of the coupling model. These results underscore the link between the JG and segmental processes, consistent with the JG relaxation functioning as the precursor to structural relaxation.

Introduction

The effect of chain length on the dynamics of polymers is an old problem^{1–3} that has nevertheless attracted substantial interest of late. While rheological properties obviously can depend strongly on molecular weight, recent studies have looked for connections between the global chain dynamics and the local segmental motions.^{4–9} Of interest herein is the effect of molecular weight, M , on segmental relaxation, along with any relation to the secondary dynamics. The most prominent segmental relaxation property is the glass transition temperature, T_g . The traditional view is that T_g is governed by the number of chain ends, based on the idea that they differ structurally from the repeat units, with the consequent ill-packing conferring excess mobility. This leads to the expectation that T_g is an increasing function of the number-average molecular weight, M_n , a quantity inversely proportional to the concentration of chain ends. Relations for linear polymers are due to Fox and Flory¹⁰

$$T_g = T_{g,\infty} - k_{FF}/M_n \quad (1)$$

and Ueberreiter and Kanig¹¹

$$T_g = (T_{g,\infty}^{-1} + k_{UK}/M_n)^{-1} \quad (2)$$

In these equations, k_{FF} and k_{UK} are constants that depend on the nature of the end groups^{12,13} and $T_{g,\infty}$ is the glass transition temperature in the absence of chain ends (i.e., high molecular weight or cyclic chains). Generally, eq 2 has been found to yield better agreement with experimental data, for example, for polyesters,¹⁴ polystyrenes,^{15,16} polysiloxanes,¹⁷ and poly(methyl methacrylate)s.¹⁸

Both expressions predict a monotonic change in T_g with chain length, in accord with general expectations, as typified by a recent analysis of Agapov and Sokolov.¹⁹ However, Roessler and co-workers^{20–22} have revived an old idea of Cowie²³ that

there are distinct regimes of $T_g(M)$ behavior. For polymers including polydimethylsiloxane, polystyrene, and 1,4-polybutadiene, they concluded that plots of T_g vs $\log M_w$ exhibit two transitions, ostensibly demarcating the onset of Rouse and entangled dynamics.²⁰ Similar behavior was reported for the T_g -normalized temperature dependence of the segmental relaxation times, τ_α ;

that is, the fragility²⁰ $m = \frac{d \log \tau_\alpha}{d(T_g/T)}$ It is surprising that the

local segmental relaxation underlying T_g should be sensitive to the global motions associated with chain dynamics, and so we examine this herein using a broad range of data for 1,4-polybutadienes (PB). Since polydispersity is common in polymers, we also assess the effect of molecular weight distribution on the segmental relaxation properties, using model PB blends. This is potentially an issue if over the distribution of chain lengths, T_g is molecular-weight-dependent. A recent study found that a large increase in molecular weight distribution increased the fragility of polystyrene,²⁴ raising the possibility that regimes in behavior could reflect competing effects of molecular weight and its distribution.

Secondary relaxations, found in small molecules as well as polymers, fall into two classes: the Johari–Goldstein (JG) relaxation and higher frequency motions. The latter are trivial, in the sense of being specific to a given material and generally having a limited effect on macroscopic properties. These higher frequency secondary relaxations are due to reorientation of some atoms in the molecule or repeat unit and include motion of a pendant group, the chain ends, particular backbone atoms, or atoms in the vicinity of crystal defects. More interesting is the JG relaxation, the lowest frequency secondary relaxation, which is present in all amorphous, glass-forming materials.^{25,26} For molecular liquids the JG process corresponds to reorientation of the entire molecule, although the rotation angle is small compared to the amplitude of structural relaxation. For polymers the dynamics of the JG process can be complicated, but is expected to involve the entire repeat unit; that is, the JG relaxation does not involve intramolecular degrees of freedom.

*To whom correspondence should be addressed.

Table 1. Polybutadienes

	PB4	PB4B ^a	PB5B ^b	PB5P ^c	PB6	PB43	PB231	PB262
vinyl content (%)	8.6				7.7	7.4	7.0	7.0
M_n (kg/mol)	3.80	4.37	4.78	5.26	6.50	43.40	231.4	262.0
M_w/M_n	1.21	2.42	13.1	1.59	1.18	1.06	1.08	1.08
T_g								
capacitance	170.3	169.0	171.2	170.1	173.0	174.5	174.8	172.8
$\tau_\alpha = 100$ s	172.1	172.7	173.1	172.9	173.2	175.2	173.9	173.7
m	90.70	93.70	105.1	89.7	88.86	99.26	101.8	99.53

^a Bimodal molecular weight distribution: 85.7% PB4 and 14.2% PB43 by weight. ^b Bimodal molecular weight distribution: 79.3% PB4 and 20.7% PB262 by weight. ^c Polydisperse: 53.4% PB4, 15.4% PB6, 16.2% PB9 ($M_n = 9.40$ kg/mol; $M_w/M_n = 1.16$), and 15.0% PB18 ($M_n = 17.6$ kg/mol; $M_w/M_n = 1.11$) by weight.

There are theoretical predictions that the shape of the segmental relaxation function, as reflected in the magnitude of the stretch exponent, β_{KWW} , in the Kohlrausch–Williams–Watts (KWW) correlation function^{27,28}

$$\Phi(t) = \exp[-(t/\tau_{KWW})^{\beta_{KWW}}] \quad (3)$$

governs both the relaxation time and the activation energy of the secondary process. (In eq 3 the time constant τ_{KWW} is approximately equal to the relaxation time τ_α defined as the inverse frequency of the maximum in the dielectric loss.) Since the secondary relaxation in 1,4-polybutadiene has a relatively large dielectric strength, these predictions can be tested with good accuracy. The results also serve to resolve an outstanding issue concerning the breadth of the segmental relaxation peak in PB.

Experimental Section

The polybutadienes were prepared by polymerizing 1,3-butadiene in anhydrous hexanes using *n*-butyllithium as the initiator. Samples were coagulated in isopropanol containing butylhydroxyl-toluene as an antioxidant, followed by drying. The vinyl content was determined by ¹H NMR and equaled $7.5 \pm 0.7\%$ (Table 1). The largest difference in vinyl content among these samples would change T_g by about 1 deg.^{29,30} Molecular weights were determined by gel permeation chromatography with a Waters WISP system and a model 410 refractometer, using tetrahydrofuran as the solvent (Mark–Houwink coefficient = 0.00145 and exponent = 0.81). Blends were prepared in cyclohexane solutions, with the solvent subsequently removed by 10 days *in vacuo* at room temperature. Samples are listed in Table 1, where the number designates M_n in kg/mol, and the suffix “P” or “B” for the blend samples refers respectively to a poly- or bidisperse molecular weight distribution.

The dielectric measurements employed a Novocontrol Alpha-A analyzer, with samples (typically 100 μ m thick) maintained between parallel capacitor plates in a closed-cycle helium cryostat under vacuum. Temperature was measured by a platinum resistance thermometer mounted in one of the electrodes. All experiments employed isothermal frequency sweeps, with 90 min soak time at each temperature prior to the measurements. Temperature stability of the cryostat is within 0.02 deg. Glass transition temperatures were defined in two ways: (i) as the temperature at which $\tau_\alpha = 100$ s, where τ_α is the inverse of the circular frequency, ω , of the dielectric loss maximum, and (ii) from the change in the slope of the capacitance vs temperature measured on temperature-equilibrated samples (isothermal measurements without rate effects). The capacitance is inversely proportional to film thickness, the latter changing due to thermal expansion; thus, this method yields a dilatometric T_g .^{31,32}

Results

Regimes of Dynamic Behavior. In Figure 1 are displayed the glass transition temperatures for the five monodisperse and three polydisperse PB. The values represent the average of the temperature at which $\tau_\alpha = 100$ s and temperature at

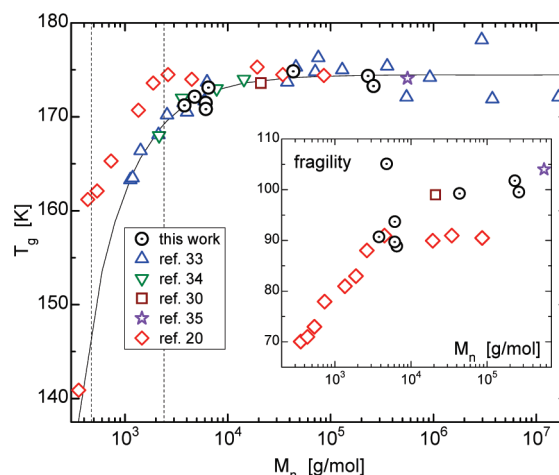


Figure 1. Glass transition temperatures measured herein (circles), representing the average of T_g determined as the temperature at which the capacitance undergoes a change in T -dependence and at which $\tau_\alpha = 100$ s. The difference between these values does not exceed the symbol size. Also shown are T_g measured by calorimetry (triangles³³ and squares³⁰), Raman scattering (inverted triangles³⁴), and dielectric spectroscopy (star³⁵). The solid line is the simultaneous fit of eq 1 to these four data sets; $T_{g,\infty} = 174.4$ K and $k_{UF} = 12.4$ kg/mol. The outlying data (diamonds²⁰) were the basis for an inference that three distinct regimes of behavior were present in PB.²⁰ The inset shows the fragility as a function of molecular weight determined in this work (circles), ref 30 (squares), ref 35 (star), and ref 20 (diamonds). Only the fragilities in ref 20, calculated from the VFTH parameters using a value of D that was the average over all molecular weights, suggest a break at the entanglement molecular weight.

which the capacitance changes its T -dependence; the two determinations are equivalent within the experimental error (Table 1). Also included are the calorimetric glass transitions for PB reported by Colby et al.,³³ the T_g determinations of Kisiuk et al.³⁴ based on the change in the T -dependence of the Raman scattering intensity, and one datum each from mechanical spectroscopy by Zorn et al.³⁰ and dielectric spectroscopy by Schroeder et al.³⁵ for $\tau_\alpha(T_g) = 100$ s. These results, encompassing 36 data points *in toto* spanning more than 4 decades of molecular weights, are well described by eq 1 (correlation coefficient = 0.92). The fit parameters, $k_{UK} = 12.4 \pm 0.9$ kg/mol and $T_{g,\infty} = 174.4 \pm 0.3$ K, are quite close to those reported in ref 33 for calorimetric T_g . There is no indication of any change in behavior at the entanglement molecular weight, $M_e \sim 1.9$ kg/mol,³ or at a lower molecular weight, $M_R \sim 0.24$ kg/mol,³⁶ corresponding to the onset of Rouse dynamics. Also shown in Figure 1 are the $T_g(M_n)$ of ref 20. These were used to support the supposition of dynamic transitions at M_e and M_R ;^{20–22} however, it can be seen that these data deviate from all other results.³⁷ The lower molecular weight polybutadienes in ref 20 had higher vinyl content (up to 20%), which may be the origin of their differing behavior.

Along with the putative regimes of $T_g(M)$, it has been suggested that the molecular weight dependence of the fragility changes at $M \sim M_c$, becoming constant at higher molecular weights,²⁰ with the data underlying this claim shown in the inset to Figure 1. It would be a provocative finding that the temperature dependence of structural relaxation was affected by the onset of topological entanglement constraints. We also show m vs M_n as measured herein, along with a single value of m reported in ref 30. The latter and our results indicate m continues to increase for $M > M_c$; the high molecular weight data cannot be fit with a straight line of zero slope. The source of the discrepancy with ref 20 is unclear, although we note that in calculating m , Hintermeyer et al.²⁰ used a value of the parameter D in the Vogel–Fulcher equation

$$\log \tau_\alpha = \log \tau_0 + \frac{D}{T - T_0} \quad (4)$$

that was the average over each D obtained by fitting each molecular weight to eq 4. Since the fragility depends strongly on this parameter

$$m = T_g \frac{D}{(T_g - T_0)^2} \quad (5)$$

(D is known as the “strength parameter”), this preaveraging of D over all M prior to calculation of m influences the obtained molecular weight dependence of these quantities. This may be the reason the change of m in ref 20 is less for large M than found herein.

Effect of Polydispersity. Notwithstanding the strong M -dependence of the rheological properties of polymers, dynamics that are more local, such as segmental relaxation, are not expected to be greatly affected by chain length beyond the influence of chain ends noted above. Thus, a secondary effect like molecular weight distribution is generally ignored in studies of the glass transition and related phenomenon in polymers. However, this is not obviously the case if the molecular weight distribution extends to values of M sufficiently low for T_g and τ_α to become molecular-weight-dependent. For example, although thermodynamically miscible polymer blends whose neat components have different T_g exhibit only one glass transition, some broadening is usually observed of both the calorimetric and relaxation peaks.³⁸ This is ascribed to dynamic heterogeneity,^{39–41} whereby the components of a miscible blend have different rates and T -dependences for their segmental dynamics, notwithstanding the homogeneity of the phase morphology.

To examine the effect of molecular weight distribution, blends were prepared from the monodisperse PB samples, with polydispersities as high as 6 obtained with a bimodal distribution of chain lengths (Table 1). The α -dispersions in the dielectric loss spectra for mono- and polydisperse samples are compared in Figure 2. (Note that T_g of the precursor polymers used to prepare the bimodal PB differ by as much as 3.6 deg, leading to differences at the measurement temperatures in their respective τ_α . This necessitated small horizontal shifting of the curves.) We find that, similar to the glass transition temperature behavior, the breadth of the segmental relaxation peak is mainly a function of M_n , with no broadening due to polydispersity. The β_{KWW} obtained from analyzing the spectra is not affected by the molecular weight distribution. In this respect the effect of molecular weight distribution differs from that of polymer blending (although the T_g differences for the latter are usually greater than herein); polydispersity only affects the concentration of chain ends, whereas the repeat units of the components

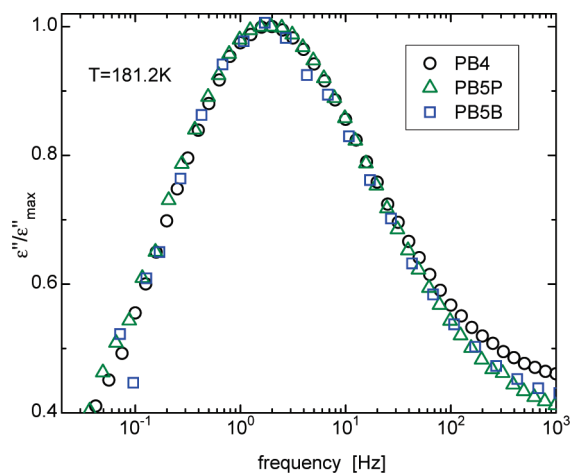


Figure 2. Segmental dispersion in the dielectric loss for three PB with narrow, broad, and bimodal molecular weight distributions. The frequencies were shifted by a factor of 2 or less to account for small difference in temperature dependence.

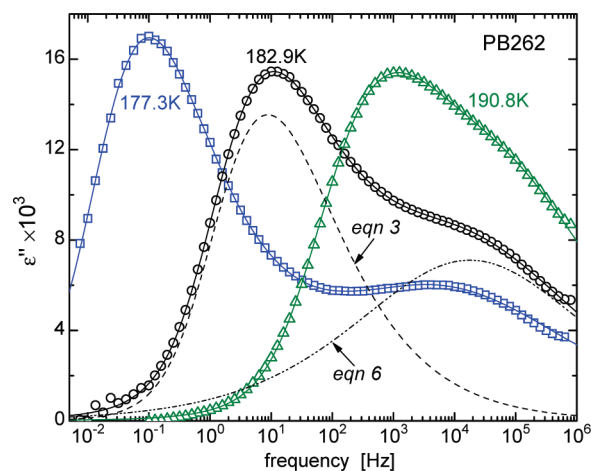


Figure 3. Representative dielectric loss for PB ($M_n = 262.0$ kg/mol) at the indicated temperatures. The solid lines are the fits obtained by addition of a KWW and Cole–Cole function; these are shown for $T = 182.9$ K as the respective dashed and dotted-dashed lines.

comprising a miscible blend have different chemical structures.

Recently, it was reported that a blend of high molecular weight polystyrene and oligomeric PS had larger fragility than a monodisperse sample having the same M_n and T_g .²⁴ In Table 1 are listed the fragilities for all PB samples herein. There is a consistent trend of increasing m with increasing M_w/M_n . The change is barely significant for the polydisperse PB6P but substantial for the samples having a bimodal molecular weight distribution.

Relationship of α - and β -Relaxations. In Figure 3 are representative dielectric loss spectra for PB267 at three temperatures, along with fits to the sum of the transform of eq 3 to describe the segmental peak and the imaginary part of the Cole–Cole function⁴²

$$\epsilon''_{cc}(\omega) = \frac{\Delta\epsilon_{cc}(\omega\tau_{cc})^{\alpha_{cc}} \sin(\alpha_{cc}\pi/2)}{1 + 2(\omega\tau_{cc})^{\alpha_{cc}} \cos(\alpha_{cc}\pi/2) + (\omega\tau_{cc})^{2\alpha_{cc}}} \quad (6)$$

to describe the JG peak. Equation 6 describes a symmetric peak (vs $\log \omega$), with $\Delta\epsilon_{cc}$, τ_{cc} , and α_{cc} as fitting parameters. With the assumption that the α - and JG-peaks contribute in additive fashion to the frequency-dependent loss, the spectra

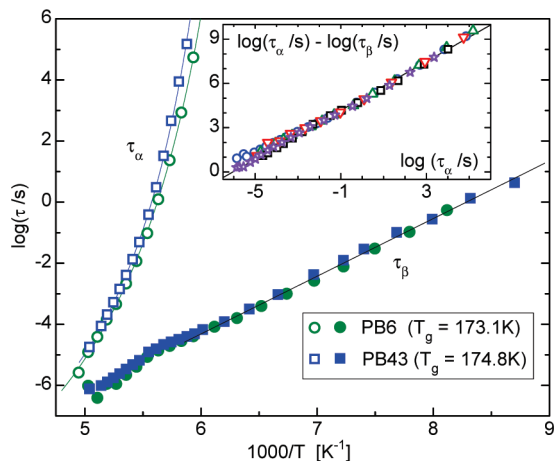


Figure 4. Relaxation times for the local segmental (open symbols) and JG secondary relaxation (filled symbols) for two monodisperse PB. For the lowest temperatures τ_α were obtained by extrapolation using time–temperature superpositioning. The solid lines are fits to eq 4 or eq 12. The inset plots the separation of the two processes for the monodisperse PB versus the segmental relaxation time; the variation is much stronger than predicted by eq 9.

could be described accurately at different temperatures, associated with varying degrees of peak overlap; this is illustrated in Figure 3.

The correctness of the assumption that the α - and secondary peaks are additive in the frequency domain has been affirmed by some reports,^{43,44} while other investigators argue that while the two processes are statistically independent, the dipoles participating in the secondary relaxation are immersed in a local environment relaxing via the α -process, so that when the two time scales are close the frequency response is not simply the addition of the two.^{45,46} A popular example of the latter approach is due to Williams,⁴⁷ who considered the relaxation of the dipoles to involve both the α - and secondary processes simultaneously, leading to the relaxation function having the form

$$\Phi(t) = f_\alpha \Phi_\alpha(t) + (1 - f_\alpha) \Phi_\alpha(t) \Phi_{JG}(t) \quad (7)$$

in which Φ_α and Φ_{JG} represent the respective relaxation functions for the α - and JG process, with f_α the relative strength of the former. Fitting the spectra in Figure 3 using eq 7 changes the value of β_{KWW} for the α -peak less than 0.002 from the result of assuming additivity in the frequency domain. Over the range of measurements herein, the difference between the two analysis methods is less than the uncertainty.

Figure 4 shows the segmental and JG relaxation times for two monodisperse PB that differ in molecular weight. Their relaxation behavior is similar, other than the different T_g and $\tau_\alpha(T)$, with the magnitude of the latter difference increasing as T is lowered. At higher temperatures (> 170 K) the T -dependence of τ_{JG} changes, as the JG relaxation begins to encroach upon the segmental process, eventually merging into a single relaxation peak. This change in behavior near T_g has been reported previously^{48–51} and underlies the idea that the JG process is the precursor of structural relaxation. Drawing on this idea, the coupling model makes a specific prediction about the JG relaxation times and their temperature dependence. According to the model⁵²

$$\log \tau_\beta = \beta_{KWW} \log \tau_\alpha + (1 - \beta_{KWW}) \log t_c \quad (8)$$

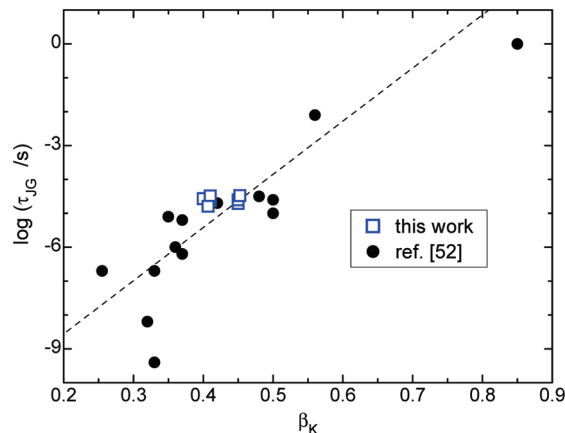


Figure 5. JG relaxation times at T_g (defined in this figure only as $\tau_\alpha = 10^4$ s) as a function of the Kohlrausch stretch exponent: PB (this work, open squares); various polymers (ref 52, filled circles). The dashed line through the data is eq 9.

where $t_c = 2 \times 10^{-12}$ s is a universal constant for organic materials. This gives for the secondary relaxation time

$$\log \tau_\beta = (11.7 + \log \tau_\alpha) \beta_{KWW} - 11.7 \quad (9)$$

Or rearranging, the separation between the primary and secondary processes is expressed as

$$\log \tau_\alpha - \log \tau_\beta = (1 - \beta_{KWW}) [\log \tau_\alpha + 11.7] \quad (10)$$

In the inset to Figure 4 the time scale separating the α - and β -processes is plotted as a function of $\log \tau_\alpha$ for the five monodisperse PB. Only at the highest temperatures, where overlap with the JG peak introduces uncertainty into the determination of β_{KWW} , is there any apparent deviation from the linear relationship predicted by eq 10. The slope of the fit is 0.81 ± 0.02 , so that eq 10 gives a value of the stretch exponent equal to 0.19. (This assumes β_{KWW} is constant, and we find herein that β_{KWW} varies by less than 0.1 over the temperature range of the measurements. A near invariance of β_{KWW} is consistent with the conformance of polybutadiene to time–temperature superpositioning when there is no interference from a secondary relaxation.⁵³) However, the experimental value of $\beta_{KWW} = 0.43 \pm 0.02$ at T_g , which is more than a factor of 2 larger than the prediction. Thus, although the expected proportionality of $\log(\tau_\alpha/\tau_\beta)$ and $\log \tau_\alpha$ is observed, an incorrect β_{KWW} is necessary to satisfy eq 10 of the coupling model. Using the experimental β_{KWW} in eq 10 gives τ_β that are 2 orders of magnitude smaller than measured. This discrepancy is beyond any uncertainty associated with the method used to deconvolute the α - and JG peaks.

Previous studies have found eqs 8–10 to be in general accord with experimental data.^{52,54} For example, in Figure 5 are results for various polymers (filled circles),⁵² showing secondary relaxation times varying in proportion to the magnitude of β_{KWW} (all data for $T = T_g$, defined as $\tau_\alpha = 10^4$ s in ref 52). The straight line is not a fit to the data but represents eq 9. The experimental $\log(\tau_\beta)$ are close to the values expected from the measured β_{KWW} , although there is substantial scatter.

A more stringent test than assessing different materials is to make systematic changes in a given material; this minimizes contributions to the experimental data from extraneous factors not accounted for by the model. Included in Figure 5 are results for the eight PB samples studied herein

Table 2. Stretch Exponent for 1,4-Polybutadiene

β_{KWW}	technique	reference
0.41	dielectric	60
0.41	dielectric	61
0.43 ± 0.02	dielectric	this work
> 0.45	mechanical	29
0.49	mechanical	30
0.52	mechanical	62
0.40	mechanical	63

(open squares), with β_{KWW} and τ_{β} for $\tau_{\alpha} = 10^4$ s, as used in ref 52. The PB data do not fall far from the calculated line; however, taken alone there is almost no variation of τ_{β} with β_{KWW} , whereas the model predicts these τ_{β} should vary by about a factor of 0.7 decade for these samples. In this respect the results are similar to an earlier study⁵⁵ in which addition of plasticizer to PB reduced T_{g} and thereby substantially reducing τ_{α} ; however, there was no significant change in either β_{KWW} or τ_{β} .

Another prediction of the coupling model concerns the relationship of the activation energy for the JG process, E_{β} , to properties of the α -relaxation⁵⁶

$$E_{\beta} = 2.303RT[(\beta_{\text{KWW}}) \log \tau_{\alpha} + (1 - \beta_{\text{KWW}}) \log t_c - \log \tau_{\beta\infty}] \quad (11)$$

in which $\tau_{\beta\infty}$ is the prefactor in the Arrhenius equation

$$\tau_{\beta}(T) = \tau_{\beta\infty} \exp(E_{\beta}/RT) \quad (12)$$

Rearranging eq 11 gives

$$E_{\beta}/RT_{\text{g}} = 2.303[-11.7 + 13.7\beta_{\text{KWW}} - \log \tau_{\beta\infty}] \quad (13)$$

Averaging the activation energies measured for the PB in the glassy state, we obtain $E_{\beta} = 36.2 \pm 0.7$ kJ/mol; this is close to an earlier value of 37.6 kJ/mol reported for a low- M_{w} PB with higher vinyl content.⁵⁷ Using our average E_{β} gives $E_{\beta}/RT_{\text{g}} = 25.1 \pm 0.4$. From the measured β_{KWW} and $\tau_{\beta\infty}$, eq 13 yields $E_{\beta}/RT_{\text{g}} = 22.7 \pm 1.1$. Thus, the coupling model prediction is somewhat less but very close to the experimental result. Note our result for PB is consistent with the empirical value $E_{\beta}/RT_{\text{g}} = 24 \pm 3$ obtained by analysis of a range of different materials.⁵⁸

Finally, we note there is a reputed controversy in the literature regarding the value of β_{KWW} for PB.⁵⁹ In Table 2 are collected the published results,^{29,30,60–63} plus our own for the eight PB samples herein. Our value, $\beta_{\text{KWW}} = 0.43 \pm 0.02$, is in good agreement with other dielectric measurements. The stretch exponent determined from mechanical spectroscopy, $\beta_{\text{KWW}} \sim 0.5$, is larger than from dielectric relaxation. This is the only apparent discrepancy among the various determinations.

Summary

From dielectric relaxation measurements on a series of polybutadienes having primarily 1,4-repeat units, the following conclusions are drawn:

1. The glass transition temperature of PB is determined by the concentration of chain ends and thus depends only on the number-average molecular weight. Putative regimes of dynamic behavior, defined by the presence of entanglement constraints or Gaussian chain behavior, are not evident in either the T_{g} or fragility results herein.

2. Polydispersity has a negligible effect on T_{g} , the shape of the segmental relaxation dispersion, and the secondary dynamics,

even when the molecular weight distribution is bimodal and extends to a range wherein T_{g} and τ_{α} become molecular-weight-dependent. The only significant effect of polydispersity was an increase of $\sim 5\%$ in the fragility for PB having a bimodal distribution.

3. The change with temperature in the time scale separating the segmental and JG relaxations is in qualitative agreement with the coupling model; however, the magnitude of this separation and thus the value of τ_{β} at T_{g} are much larger than the values predicted by the model. On the other hand, the model's prediction for the activation energy of the JG process is close to the experimentally determined E_{β} .

Acknowledgment. R.B.B. is grateful for an ASEE postdoctoral fellowship. We thank Daniel Fragiadakis, who wrote the software to implement eq 7. The work at NRL was supported by the Office of Naval Research.

References and Notes

- Flory, P. J. *Principles of Polymer Chemistry*; Cornell University Press: Ithaca, NY, 1953.
- Ferry, J. D. *Viscoelastic Properties of Polymers*; Wiley: New York, 1980.
- Rubinstein, M.; Colby, R. H. *Polymer Physics*; Oxford University Press: Oxford, 2003.
- Sokolov, A. P.; Schweizer, K. S. *Phys. Rev. Lett.* **2009**, *102*, 248301.
- Ding, Y.; Sokolov, A. P. *Macromolecules* **2006**, *39*, 3322.
- Ngai, K. L.; Plazek, D. J.; Roland, C. M. *Phys. Rev. Lett.* **2009**, *103*, 159801.
- Ngai, K. L.; Plazek, D. J.; Roland, C. M. *Macromolecules* **2008**, *41*, 3925.
- Roland, C. M.; Ngai, K. L.; Plazek, D. J. *Macromolecules* **2004**, *37*, 7051.
- Liu, C.; Li, C.; Chen, P.; He, J.; Fan, Q. *Polymer* **2004**, *45*, 2803.
- Fox, T. G.; Flory, P. J. *J. Polym. Sci.* **1954**, *14*, 315.
- Ueberreiter, K.; Kanig, G. *J. Colloid Sci.* **1952**, *7*, 569.
- Turner, D. T. *Polymer* **1978**, *19*, 789.
- Danusso, F.; Levi, M.; Gianotti, G.; Turri, S. *Polymer* **1993**, *34*, 3687.
- Montserrat, S.; Colomer, R. *Polym. Bull.* **1984**, *12*, 173.
- Aras, L.; M.J. Richardson, M. J. *Polymer* **1984**, *30*, 2246.
- Robertson, C. G.; Roland, C. M. *J. Polym. Sci., Part B: Polym. Phys.* **2004**, *42*, 2604.
- Cowie, J. M. G. *Polymer* **1973**, *14*, 423.
- Kusy, R. P.; Simmons, W. F.; Greenberg, A. R. *Polymer* **1981**, *22*, 268.
- Agapov, A. L.; Sokolov, A. P. *Macromolecules* **2009**, *42*, 2877.
- Hintermeyer, J.; Herrmann, A.; Kahlau, R.; Goiceanu, C.; Rossler, E. A. *Macromolecules* **2008**, *41*, 9335.
- Kariyo, S.; Brodin, A.; Gainaru, C.; Herrmann, A.; Hintermeyer, J.; Schick, H. *Macromolecules* **2008**, *41*, 5322.
- Kariyo, S.; Gainaru, C.; Schick, H.; Brodin, A.; Novikov, V. N.; Rossler, E. A. *Phys. Rev. Lett.* **2006**, *97*, 207803.
- Cowie, J. M. G. *Eur. Polym. J.* **1975**, *11*, 297.
- Dalle-Ferrier, C.; Simon, S.; Zheng, W.; Badrinarayanan, P.; Fennell, T.; Frick, B.; Zanolli, J. M.; Alba-Simionesco, C. *Phys. Rev. Lett.* **2009**, *103*, 185702.
- Bershtein, V. A.; Yegorov, V. M. *Polym. Sci. USSR* **1985**, *27*, 2743.
- Ngai, K. L.; Paluch, M. J. *J. Chem. Phys.* **2004**, *120*, 857.
- Kohlrausch, R. *Ann. Phys.* **1847**, *12*, 393.
- Williams, G.; Watts, D. C. *Trans. Faraday Soc.* **1970**, *66*, 80.
- Roland, C. M.; Ngai, K. L. *Macromolecules* **1991**, *24*, 5315.
- Zorn, R.; McKenna, G. B.; Willner, L.; Richter, D. *Macromolecules* **1995**, *28*, 8552.
- McCammom, R. D.; Work, R. N. *Rev. Sci. Instrum.* **1965**, *36*, 1169.
- Bauer, C.; Bohmer, R.; Moreno-Flores, S.; Richert, R.; Sillescu, H.; Neher, D. *Phys. Rev. E* **2000**, *61*, 1755.
- Colby, R. H.; Fetters, L. J.; Graessley, W. W. *Macromolecules* **1987**, *20*, 2226.
- Kisliuk, A.; Ding, Y.; Hwang, J.; Lee, J. S.; Annis, B. K.; Foster, M. D.; Sokolov, A. P. *J. Polym. Sci., Polym. Phys.* **2002**, *40*, 2431.
- Schroeder, M. J.; Ngai, K. L.; Roland, C. M. *J. Polym. Sci., Polym. Phys. Ed.* **2006**, *45*, 342.

- (36) Klein, P. G.; Adams, C. H.; Brereton, M. G.; Ries, M. E.; Nicholson, T. M.; Hutchings, L. R.; Richards, R. W. *Macromolecules* **1998**, *31*, 8871.
- (37) The polybutadiene in ref 20 was initiated with *sec*-butyllithium, whereas *n*-butyl was used herein; thus, there is a small difference in the nature of one of the end groups for the polymers in these two studies.
- (38) Roland, C. M. *Macromolecules* **1987**, *20*, 2557.
- (39) Alegria, A.; Colmenero, J.; Ngai, K. L.; Roland, C. M. *Macromolecules* **1994**, *27*, 4486.
- (40) Miller, J. B.; McGrath, K. J.; Roland, C. M.; Trask, C. A.; Garroway, A. N. *Macromolecules* **1990**, *23*, 4543.
- (41) Colby, R. H. *Polymer* **1989**, *30*, 1275.
- (42) Cole, K. S.; Cole, R. H. *J. Chem. Phys.* **1941**, *9*, 341.
- (43) Donth, E.; Schroter, K.; Kahle, S. *Phys. Rev. E* **1999**, *60*, 1099.
- (44) Garwe, F.; Schonhals, A.; Lockwenz, H.; Beiner, M.; Schroter, K.; Donth, E. *Macromolecules* **1996**, *29*, 247.
- (45) Arbe, A.; Colmenero, J.; Gomez, D.; Richter, D.; Farago, B. *Phys. Rev. E* **1999**, *60*, 1103.
- (46) Bergman, R.; Alvarez, F.; Alegria, A.; Colmenero, J. *J. Chem. Phys.* **1998**, *109*, 7546.
- (47) Williams, G. *Adv. Polym. Sci.* **1979**, *33*, 60.
- (48) Wagner, H.; Richert, R. *J. Phys. Chem. B* **1999**, *103*, 4071.
- (49) Fujima, T.; Frusawa, H.; Ito, K. *Phys. Rev. E* **2002**, *66*, 031503.
- (50) Nozaki, R.; Zenitani, H.; Minoguchi, A.; Kitai, K. *J. Non-Cryst. Solids* **2002**, *307–310*, 349.
- (51) Paluch, M.; Roland, C. M.; Pawlus, S.; Ziolo, J.; Ngai, K. L. *Phys. Rev. Lett.* **2003**, *91*, 115701.
- (52) Ngai, K. L. *J. Chem. Phys.* **1998**, *109*, 6982.
- (53) Zorn, R.; Mopsik, F. I.; McKenna, G. B.; Willner, L.; Richter, D. *J. Chem. Phys.* **1997**, *107*, 3645.
- (54) Capaccioli, S.; Prevosto, D.; Kessairi, K.; Lucchesi, M.; Rolla, P. *J. Non-Cryst. Solids* **2007**, *353*, 3984.
- (55) Casalini, R.; Ngai, K. L.; Robertson, C. G.; Roland, C. M. *J. Polym. Sci., Polym. Phys. Ed.* **2000**, *38*, 1841.
- (56) Ngai, K. L.; Capaccioli, S. *Phys. Rev. E* **2004**, *69*, 031501.
- (57) Deegan, R. D.; Nagel, S. R. *Phys. Rev. B* **1995**, *52*, 5653.
- (58) Kudlik, A.; Benkhof, S.; Blochowicz, T.; Tschirwitz, C.; Roessler, E. *J. Mol. Struct.* **1999**, *479*, 201.
- (59) Phillips, J. C. arXiv:0903.1067, **2009**.
- (60) Arbe, A.; Richter, D.; Colmenero, J.; Farago, B. *Phys. Rev. E* **1996**, *54*, 3853.
- (61) Hofmann, A.; Alegria, A.; Colmenero, J.; Willner, L.; Buscaglia, E.; Hadjischristidis, N. *Macromolecules* **1996**, *29*, 129.
- (62) Robertson, C. G.; Roland, C. M. *Macromolecules* **2000**, *33*, 1262.
- (63) Palade, L. I.; Verney, V.; Attane, P. *Macromolecules* **1995**, *28*, 7051.